

## Supplementary information

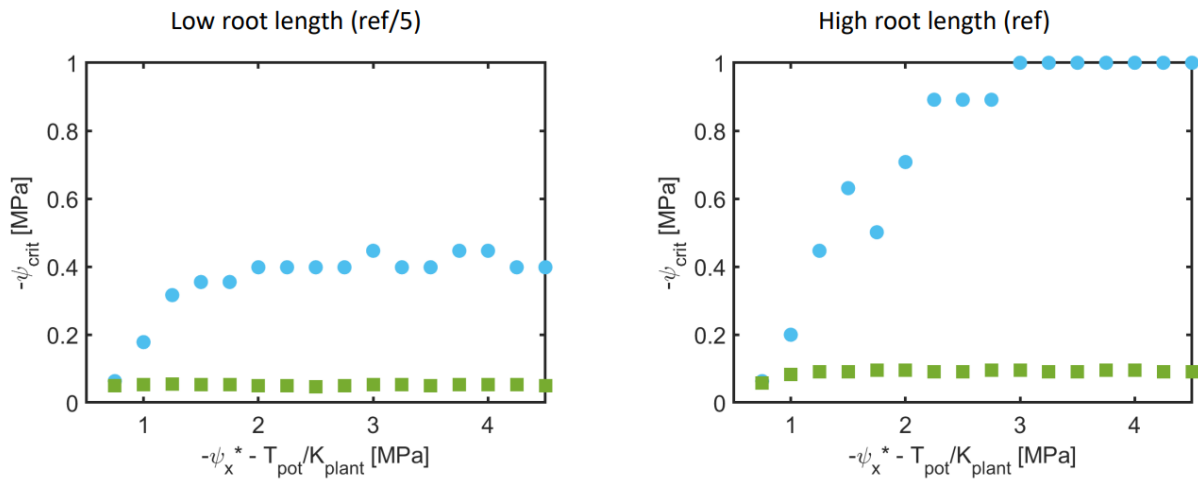
---

# Global influence of soil texture on ecosystem water limitation

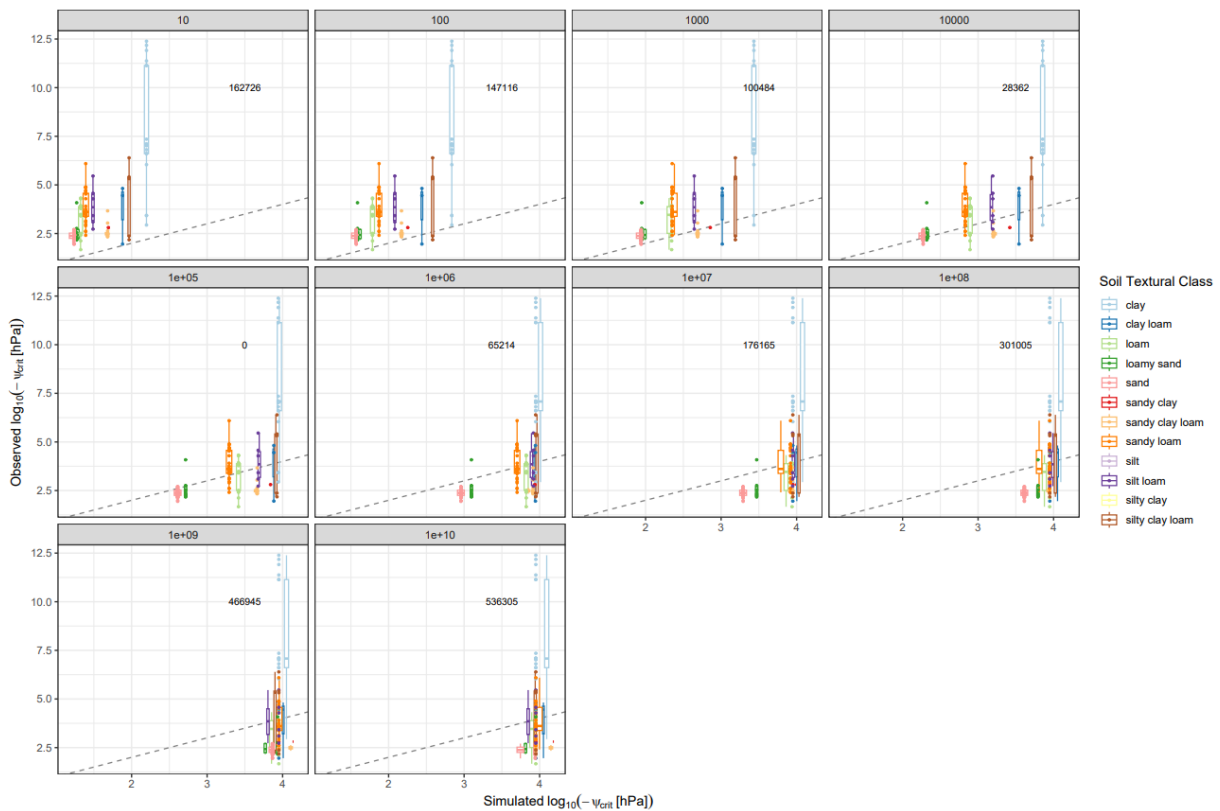
---

In the format provided by the authors and unedited

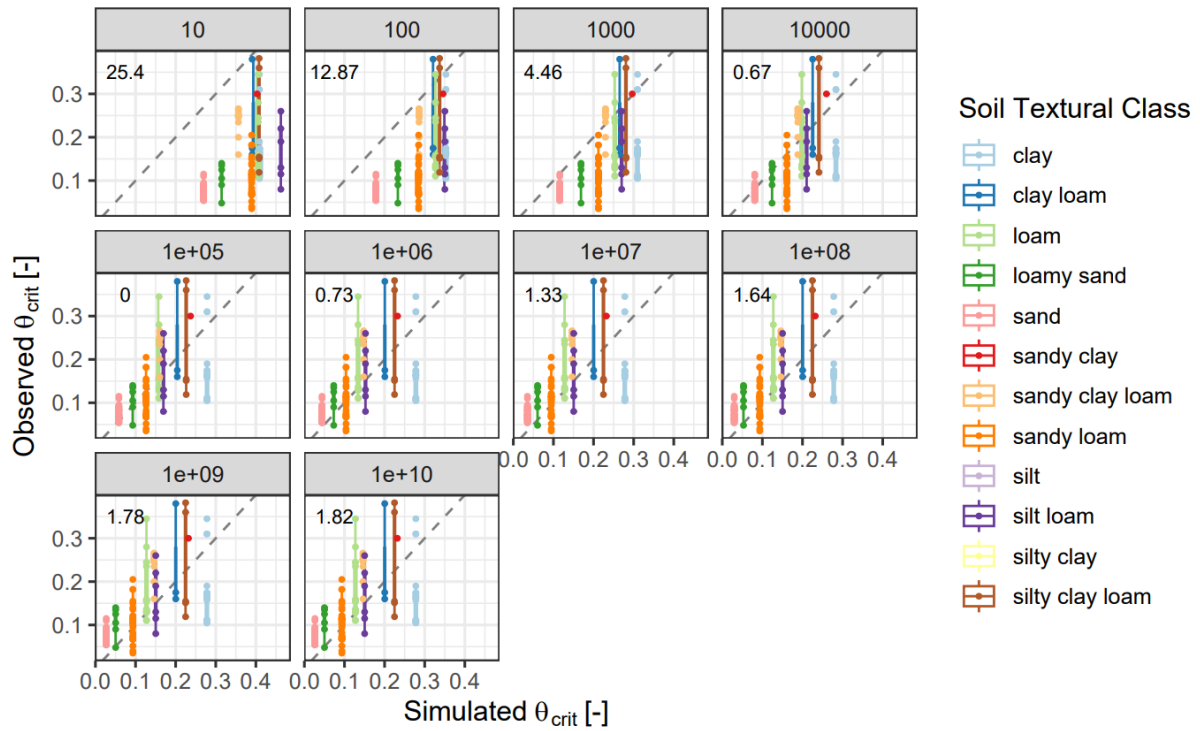
# 1 SUPPLEMENTARY INFORMATION



2  
3 **Fig. S1 | Sensitivity of  $\psi_{crit}$  on plant traits across two contrasting soil textures (clay in blue and loamy sand in green)**  
4 **for two root lengths (the reference one used for the simulations of Fig2 and one with 5 times less roots).**  $\psi_x^*$  is the plant  
5 water potential threshold at which plant conductance drops (e.g. due to cavitation). A key variable to explain the sensitivity of  
6  $\psi_{crit}$  to soil texture is:  $-T_{max}/K_{plant} - \psi_x^*$ . When it is low ( $< ca. 1$  MPa), plants limit transpiration and there are no effects of soil  
7 texture on  $\psi_{crit}$ . The effects of soil texture are visible when  $-T_{max}/K_{plant} - \psi_x^* > 1$  MPa.



8  
9 **Fig. S2 | Sensitivity of  $\psi_{crit}$  on the effective root length  $L_{root}$ .** Changing  $L_{root}$  from 10 to  $1e+10$  cm  $m^{-2}$  (titles to each panel)  
10 results in variable soil texture dependence of  $\psi_{crit}$ , i.e. it shows how extraordinary root lengths ( $\sim L_{root}$  inf.) result in simulated  
11  $\psi_{crit}$  being independent from soil texture and converging towards the plant water potential threshold ( $\psi_x^*$ ), see also Fig.1d and  
12 Fig. S3.



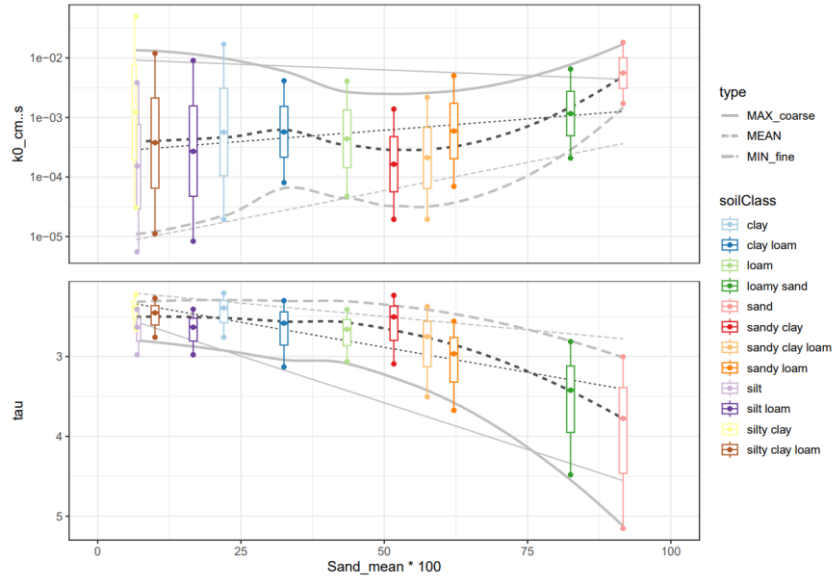
13  
 14 **Fig. S3 | Sensitivity of  $\theta_{crit}$  on the effective root length  $L_{root}$ .** Changing  $L_{root}$  from 10 to  $1e+10$   $cm\ m^{-2}$  (titles to each panel)  
 15 shows how well simulated  $\theta_{crit}$  fit to observed  $\theta_{crit}$  (particularly bad for short roots). See also Fig. S4 for comparison.

16 **Table S1 | Hydraulic properties of the soil textural classes used for the calculations of the critical water content  $\theta_{crit}$ .**  
 17 Saturated  $\theta_{sat}$  and residual water content  $\theta_{res}$ , shape parameter  $l$ , and air-entry value  $h_b$  according to the Brooks and Corey  
 18 model were chosen from <sup>77</sup>. The power-law exponent of the conductivity function  $\alpha$  was set to  $\alpha = 3l+2$ . For the saturated  
 19 hydraulic conductivity  $K_{sat}$ , the values of <sup>77</sup>,  $K_{sat}^a$ , and <sup>78</sup>,  $K_{sat}^b$ , are listed. For the simulations of  $\theta_{crit}$ , data from <sup>78</sup> were used  
 20 due to the larger data set and given that variation of  $K_{sat}$  were provided (missing in <sup>77</sup>). Note that <sup>77</sup> did not list silt soil textural  
 21 class and we chose the same values as for silt loam (as it is proposed in Hydrus software).

Soil Textural Class	$\theta_{sat}$ [cm <sup>3</sup> cm <sup>-3</sup> ]	$\theta_{res}$ [cm <sup>3</sup> cm <sup>-3</sup> ]	$l$ [-]	$t$ [-]	$h_b$ [cm]	$K_{sat}^a$ [cm h <sup>-1</sup> ]	$K_{sat}^b$ [cm h <sup>-1</sup> ]	No. of fluxnet sites per class	No. of sapfluxnet sites per class
sand	0.437	0.020	0.592	3.776	7.26	21.00	20.08	5	4
loamy sand	0.437	0.035	0.474	3.422	1.80	6.11	4.18	6	0
sandy loam	0.453	0.041	0.322	2.966	3.45	2.59	2.13	9	4
loam	0.463	0.027	0.220	2.660	1.63	1.32	1.58	3	2
silt loam	0.501	0.015	0.211	2.633	3.58	0.68	0.97	6	0
sandy clay loam	0.398	0.068	0.250	2.750	5.57	0.43	0.76	3	1
clay loam	0.464	0.075	0.194	2.582	5.80	0.23	2.06	3	0
silty clay loam	0.471	0.040	0.151	2.453	6.68	0.15	1.36	1	1

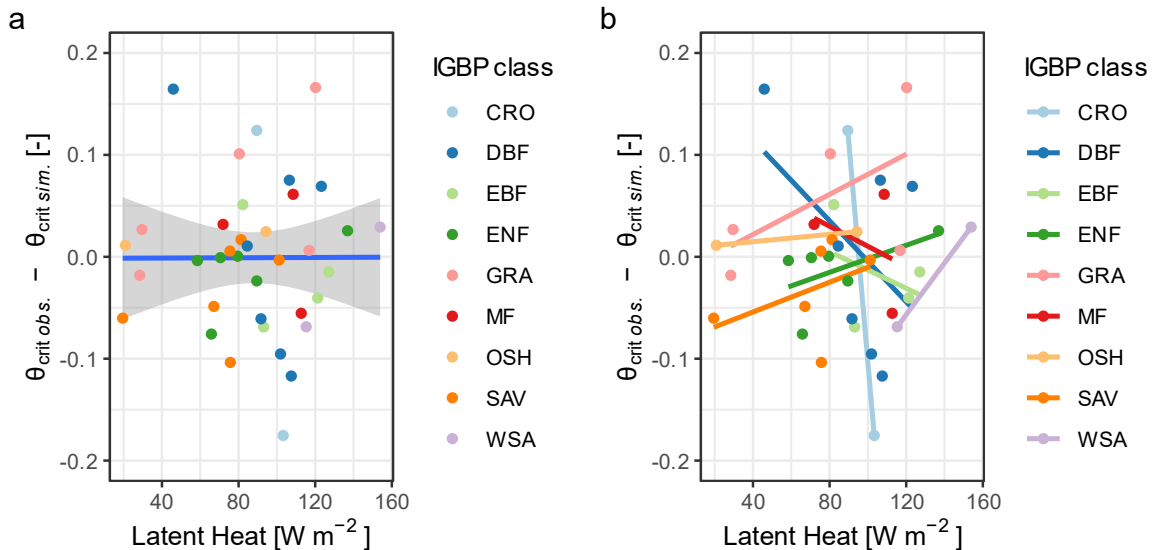
sandy clay	0.430	0.109	0.168	2.504	4.96	0.12	0.59	1	0
silty clay	0.479	0.056	0.127	2.381	7.04	0.09	4.42	0	0
clay	0.475	0.090	0.131	2.393	7.43	0.06	2.03	6	2
silt	0.501	0.015	0.211	2.633	3.58	0.68	0.55	0	0

22



23

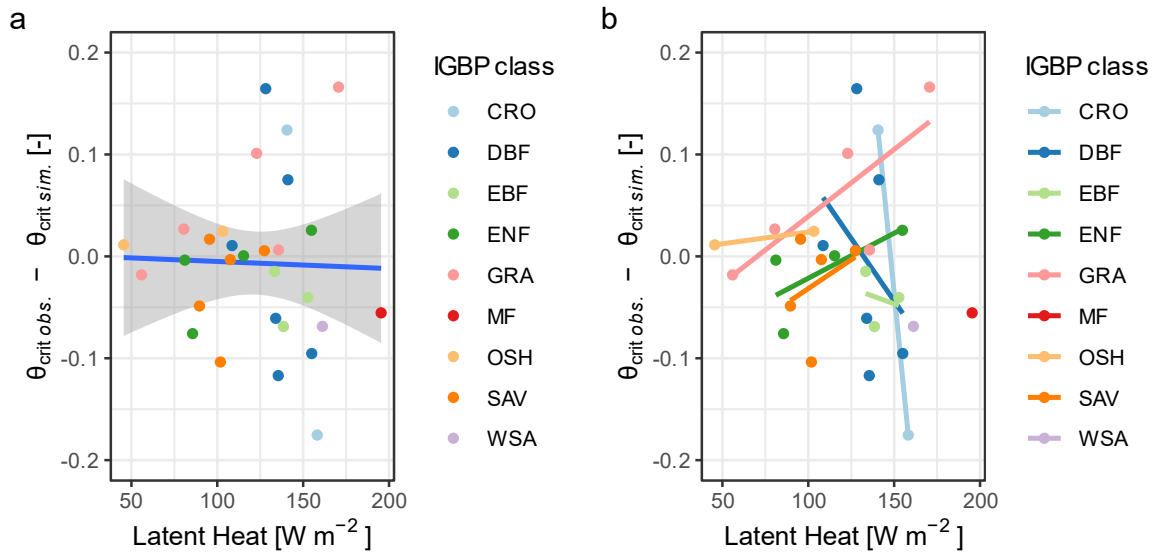
24 **Fig. S4 | Visualization of the variability of two key soil hydraulic properties.** Variability of saturated hydraulic conductivity  
 25 ( $k0_{cm.s}$ ,  $cm\ s^{-1}$ ) and the slope of the unsaturated hydraulic conductivity curve ( $\tau$ ) within a soil textural class plotted against  
 26 the mean sand fraction ( $Sand\_mean * 100$ , %). See the methods section for description how the variability of soil texture class-  
 27 specific hydraulic properties was derived.



28

29 **Fig. S5 | Simulated fluxnet  $\theta_{crit}$  do not show systematic deviation from observed  $\theta_{crit}$  across climates and biomes.**  
 30 Relationships of the differences between observed (fluxnet) and simulated  $\theta_{crit}$  to site-specific latent heat fluxes (i.e., to the  
 31 absolute evapotranspiration rates determined by the climate of each site;  $T_{pot}$ ) across climates and biomes using the average  
 32 latent heat flux in the EF-plateau above  $\theta_{crit}$ .

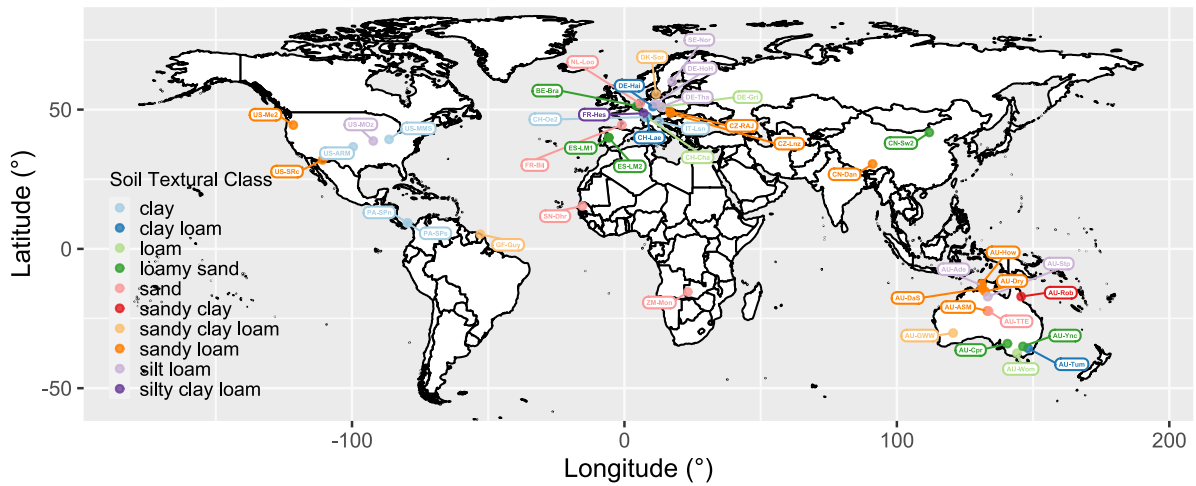
33



35

36 **Fig. S6 | Simulated fluxnet  $\theta_{crit}$  do not show systematic deviation from observed  $\theta_{crit}$  across climates and biomes.**  
 37 Relationships of the differences between observed (fluxnet) and simulated  $\theta_{crit}$  to site-specific latent heat fluxes (i.e., to the  
 38 absolute evapotranspiration rates determined by the climate of each site;  $T_{pot}$ ) across climates and biomes using the  
 39 ‘envelope’ of latent heat fluxes in the EF-plateau above  $\theta_{crit}$ .

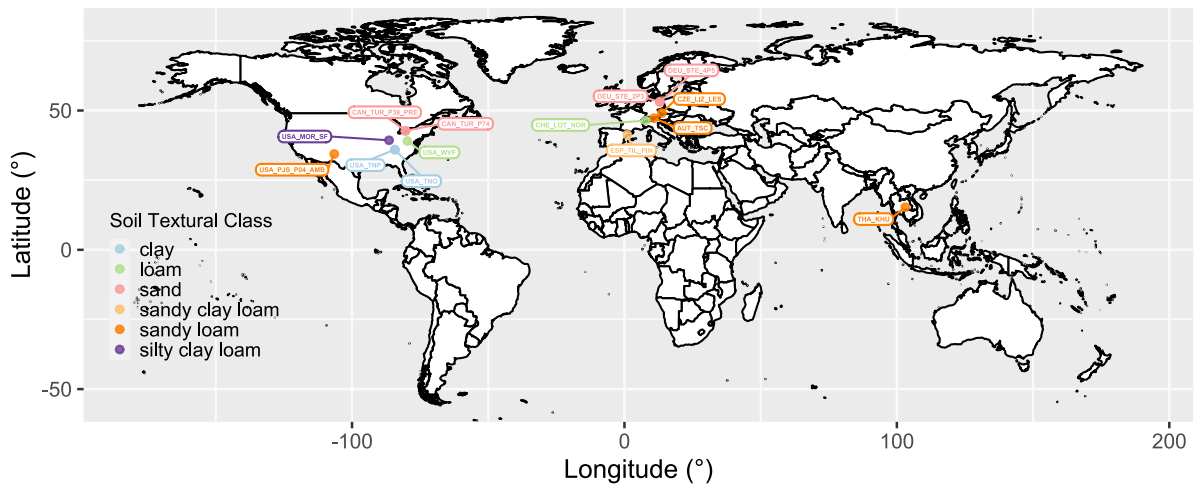
40



41

42 **Fig. S7 | Locations of the FLUXNET Eddy-Covariance sites included in this study.**

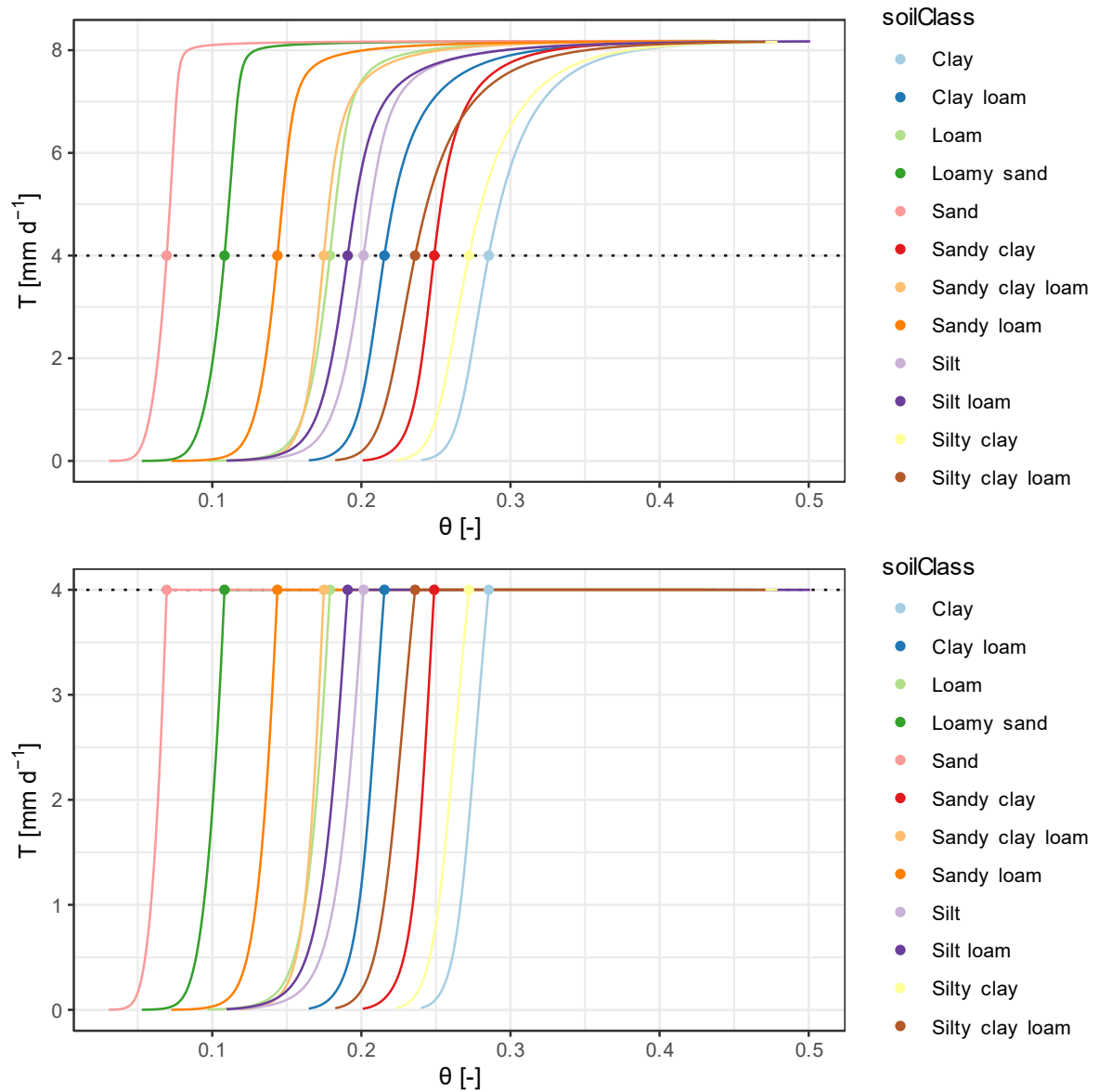
43



44

45

Fig. S8 | Locations of the SAPFLUXNET sites included in this study.



46

47 **Fig. S9 | Numerical  $T(\theta)$  functions used for the analysis on the global sensitivity of critical soil moisture thresholds to**  
48 **climate change.** Note that the model parameters used in this simulation were slightly different from the default parameter  
49 values used in the main analysis of the manuscript (Table S1), but differences in  $\Delta\theta_{crit}/\Delta T_{pot}$  around  $\theta_{crit}$  between this simulation  
50 run and the default simulation are negligible in relation to the uncertainties originating from this simplified analysis of climate  
51 change impacts (i.e. considering solely the effect of VPD on critical soil water thresholds). Here,  $\psi_{leaf-max} = -0.5$  MPa,  $\psi_{x*} = -2$   
52 MPa, and  $L_{root} = 320 \text{ m m}^{-2}$  as it was fitted to FLUXNET data only (true ecosystem scale flux data). Note that these parameters  
53 ensured that the  $T(\theta)$  functions did not yet reach their hydraulically restricted plateau in the range of VPD increases projected  
54 by the considered climate scenario for 2060-2069 ( $T_{pot} +65\% = 6.6 \text{ mm d}^{-1}$ ), whereas the default parameter values (Table S1)  
55 would hydraulically limit the transpiration rate beforehand.

56 **Table S2** | Site identifier (Site ID), data type (EC: Eddy Covariance, SF: Sapflow), continent, latitude (Lat, °), longitude (Long, °), IGBP land cover class (IGBP), mean annual temperature (MAT, °C) or temperature range (TR, °C) when MAT is not available, mean annual precipitation (MAP, mm), average site-specific latent heat flux where  $\theta > \theta_{crit}$ , fluxnet only (LE\_avg, W m<sup>-2</sup>), study  
57 periods (Periods), locally measured fractions of sand silt and clay (Sand|Silt|Clay, %) where available, soil textural class (soil texture) classified according to USDA where applicable, estimated soil  
58 moisture threshold ( $\theta_{crit}$ , %), median per sapfluxnet site, and references (Ref) of eddy covariance sites used in the study. Abbreviations: WSA, Woody Savannah; SAV, Savannah; EBF, Evergreen  
59 Broadleaf Forests; GRA, Grasslands; MF, Mixed Forests; CRO, Croplands; ENF, Evergreen Needleleaf Forests; DBF, Deciduous Broadleaf Forests; OSH, Open Shrublands.  
60

61

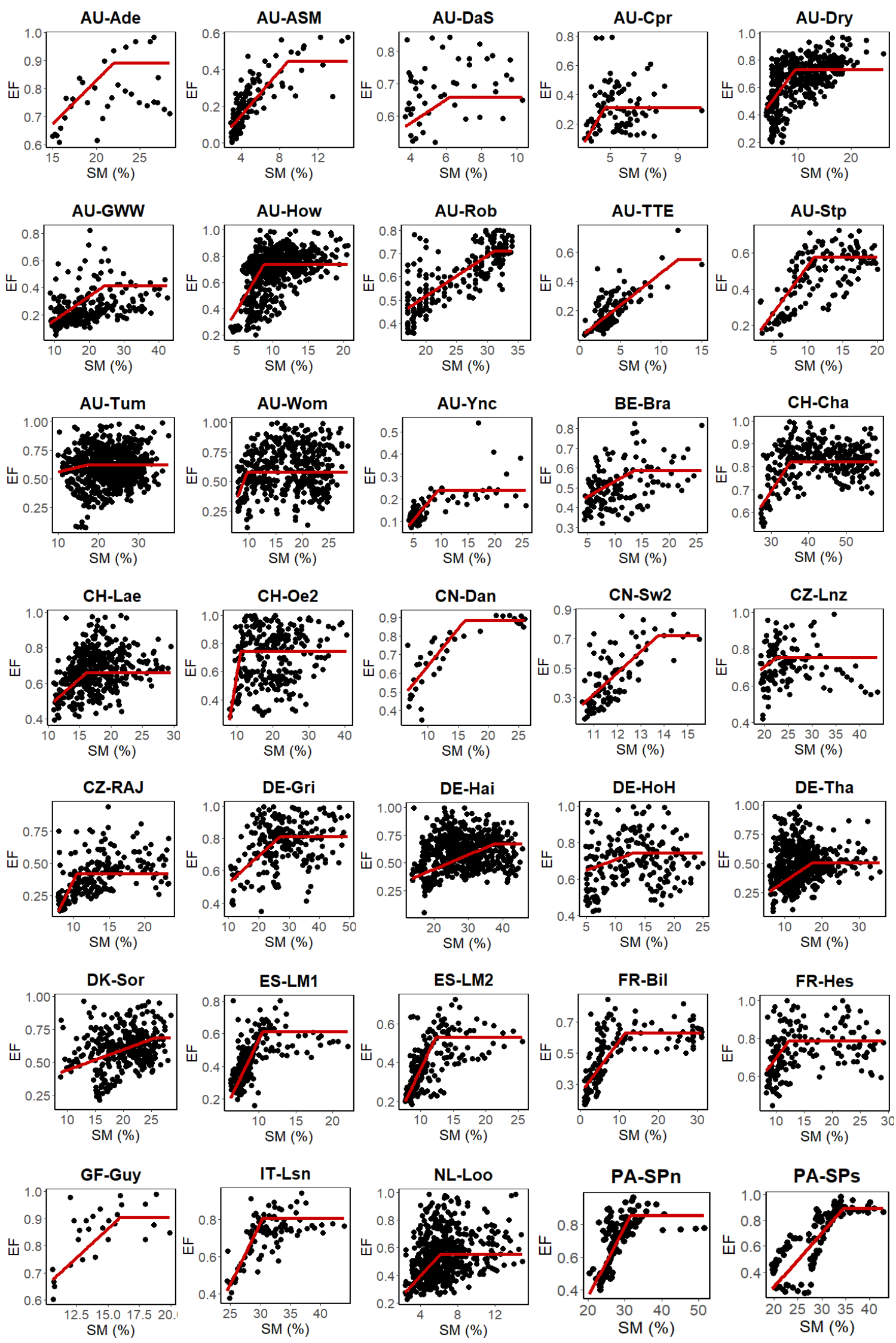
ID	Site ID	Data Type	Continent	Lat	Long	IGBP	MAT	MAP	LE_avg	Periods	Sand Silt Clay	Soil texture	$\theta_{crit}$	Ref
							(TR)							
1	AU-Ade	EC	Oceania	-13.08	131.12	WSA	(16 – 36)	1730	153.9	2007-2009		Silt loam	22	88
2	AU-ASM	EC	Oceania	-22.28	133.25	SAV	(-4 – 46)	305.09	67.1	2010-2014	74 11 15	Sandy loam	9.5	89
3	AU-Cpr	EC	Oceania	-34.00	140.59	SAV	(12 – 45)	240	19.5	2010-2014		Loamy sand	4.8	90
4	AU-DaS	EC	Oceania	-14.16	131.39	SAV	27.22	975.82		2008-2014		Sandy loam	3.5	91
5	AU-Dry	EC	Oceania	-15.26	132.37	SAV	(14 – 37)	895	75.7	2008-2014		Sandy loam	4	92
6	AU-GWW	EC	Oceania	-30.19	120.65	SAV	(5 – 33)	240		2013-2014	57 15 28	Sandy clay loam	20	93
7	AU-How	EC	Oceania	-12.49	131.15	WSA	27.01	1449.35	115.3	2001-2014		Sandy loam	7.5	94
8	AU-Rob	EC	Oceania	-17.12	145.63	EBF	(3 – 33)	2236	82.2	2014-2014	46 18 36	Sandy clay	30	95
9	AU-Stp	EC	Oceania	-17.15	133.35	GRA	(11 – 39)	640		2008-2014		Silt loam	8	96
10	AU-TTE	EC	Oceania	-22.29	133.64	GRA	(-4 – 46)	305		2012-2014	91 8 1	Sand	11	97
11	AU-Tum	EC	Oceania	-35.66	148.15	EBF	10.72	1159.01	121.3	2001-2014		Clay loam	17.5	98
12	AU-Wom	EC	Oceania	-37.42	144.09	EBF	(1 – 30)	650	93.1	2010-2014	45 29 26	Loam	11	99
13	AU-Ync	EC	Oceania	-34.99	146.29	GRA	(12 – 37)	465	28.4	2012-2014		Loamy sand	9	100
14	BE-Bra	EC	Europe	51.31	4.52	MF	9.8	750	71.9	1996-2018		Loamy sand	14	101

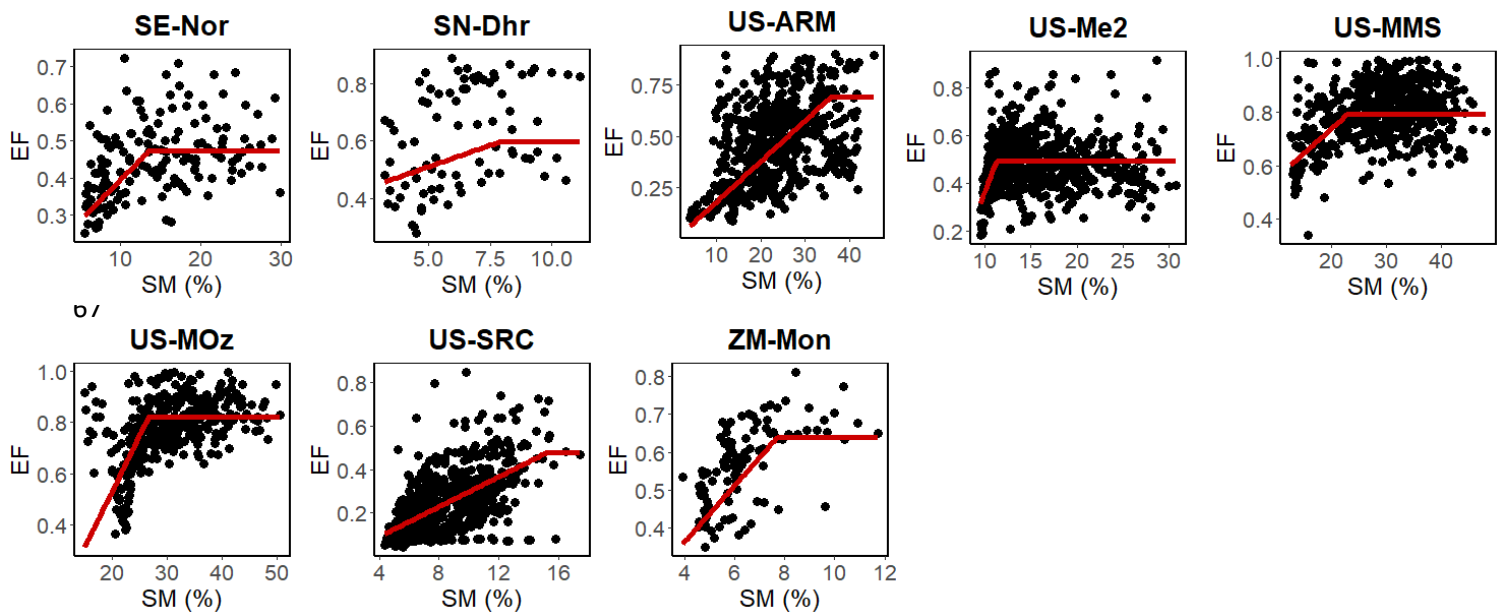


15	CH-Cha	EC	Europe	47.21	8.41	GRA	9.5	1136	120.2	2005-2018		Loam	34.5	102
16	CH-Lae	EC	Europe	47.48	8.36	MF	8.3	1100	112.7	2004-2018		Clay loam	16	103
17	CH-Oe2	EC	Europe	47.29	7.73	CRO	9.8	1155	103.3	2004-2018	25 33 42	Clay	11	104
18	CN-Dan	EC	Asia	30.50	91.07	GRA	-1.54	246.88	116.8	2004-2005	67 18 15	Sandy loam	15	105
19	CN-Sw2	EC	Asia	41.79	111.90	GRA	3.4	180	29.6	2010-2012		Loamy sand	13.5	106
20	CZ-Lnz	EC	Europe	48.68	16.95	MF	9.80	518.03	108.5	2015-2018		Sandy loam	20.5	107
21	CZ-RAJ	EC	Europe	49.44	16.70	ENF	7.1	681	58.5	2012-2018		Sandy loam	14	108
22	DE-Gri	EC	Europe	50.95	13.51	GRA	7.8	901	80.4	2004-2018		Loam	28	109
23	DE-Hai	EC	Europe	51.08	10.45	DBF	8.3	720	45.9	2000-2018		Clay loam	38	110
24	DE-HoH	EC	Europe	52.09	11.22	DBF	9.1	563	91.7	2015-2018		Silt loam	13	111
25	DE-Tha	EC	Europe	50.96	13.57	ENF	8.2	843	70.5	1996-2018		Silt loam	19	112
26	DK-Sor	EC	Europe	55.59	11.64	DBF	8.2	660	106.5	1996-2018		Sandy clay loam	25	113
27	ES-LM1	EC	Europe	39.94	-5.78	SAV	16	700	101.2	2014-2018		Loamy sand	10.5	114
28	ES-LM2	EC	Europe	39.93	-5.78	SAV	16	700	81.3	2014-2018		Loamy sand	12.5	114
29	FR-Bil	EC	Europe	44.49	-0.96	ENF	12.8	930	136.9	2014-2018		Sand	9.5	115
30	FR-Hes	EC	Europe	48.67	7.06	DBF	9.2	820	107.5	2014-2018		Silty clay loam	11.9	116
31	GF-Guy	EC	South America	5.28	-52.92	EBF	25.7	3041	127.1	2004-2014	48-64  -  43-26	Sandy clay loam	16	117
32	IT-Lsn	EC	Europe	45.75	12.75	OSH	13.1	1083	94.3	2016-2018		Clay	31	111

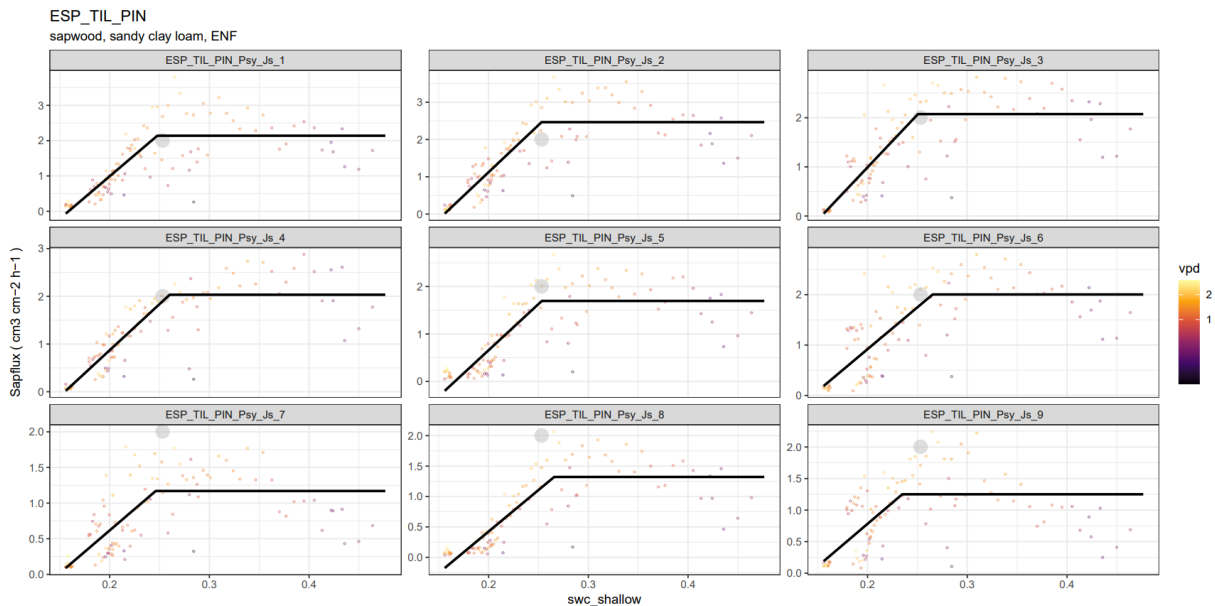
33	NL-Loo	EC	Europe	52.17	5.74	ENF	9.8	786	79.5	1996-2018		Sand	7	118
34	PA-SPn	EC	South America	9.32	-79.63	DBF	26.5	2350		2007-2009	4 30 65	Clay	31	119
35	PA-SPs	EC	South America	9.31	-79.63	DBF	26.5	2350		2007-2009	4 30 65	Clay	34.5	119
36	SE-Nor	EC	Europe	60.09	17.48	ENF	5.5	527	65.8	2014-2018		Silt loam	11.5	111
37	SN-Dhr	EC	Europe	15.40	-15.43	SAV	29	404	75.5	2010-2013	95 4.6 0.4	Sand	7.5	120
38	US-ARM	EC	North America	36.64	-99.60	CRO	14.76	843	89.5	2003-2020	28 29 43	clay	36	121
39	US-Me2	EC	North America	44.45	-121.56	ENF	6.28	523	89.5	2002-2020	67 26 7	Sandy loam	12	122
40	US-MMS	EC	North America	39.32	-86.41	DBF	10.85	1032	101.9	1999-2020	34 3 63	Clay	19	123
41	US-MOz	EC	North America	38.74	-92.20	DBF	12.11	986	123.2	2004-2019		Silt loam	26	124
42	US-SRc	EC	North America	31.91	-110.84	OSH	22	330	20.9	2008-2014		Sandy loam	15.5	125
43	ZM-Mon	EC	Africa	-15.44	23.25	DBF	25	945	84.5	2000-2009	97.5 1.9 0.6	Sand	8	126
44	AUT_TSC	SF	Europe	47.23	10.84	ENF	8.5	694		2012	54 44 2	sandy loam	6.8	<a href="mailto:walter.oberhuber@uibk.ac.at">walter.oberhuber@uibk.ac.at</a> , <a href="mailto:gerhard.wieser@uibk.ac.at">gerhard.wieser@uibk.ac.at</a>
45	CAN_TUR_P39_PRE	SF	North America	42.71	-80.36	ENF	9	1000		2008-2016	98 1 1	sand	8.9	127
46	CAN_TUR_P74	SF	North America	42.71	-80.35	ENF	9	1003		2008-2016	98 1 1	sand	8.1	127
47	CHE_LOT_NOR	SF	Europe	46.39	7.76	ENF	5	716		2006-2015	48 42 10	loam	13.6	128
48	CZE_LIZ_LES	SF	Europe	49.07	13.68	ENF	6	837		2007-2009	60.75 30.98 8.27	sandy loam	18.2	129
49	DEU_STE_2P3	SF	Europe	53.1	13	DBF	8.9	595		2002-2003	92.5 5 2.5	sand	5.8	130
50	DEU_STE_4P5	SF	Europe	53.1	13	DBF	8.9	595		2004-2005	92.5 5 2.5	sand	6.4	130
51	ESP_TIL_PIN	SF	Europe	41.33	1.01	ENF	10.1	674		2005-2011	60 20 20	sandy clay loam	25.3	131

52	THA_KHU	SF	Asia	15.27	103.08	DBF	27.2	1178		2006-2008	65 25 10	sandy loam	11.1	<sup>132</sup>
53	USA_MOR_SF	SF	North America	39.32	-86.41	DBF	12	1159		2011-2013	10 60 30	silty clay loam	15.5	<sup>133</sup>
54	USA_PJS_P04_AMB	SF	North America	34.39	-106.53	WSA	12.7	311		2006-2015	52 42 6	sandy loam	10.7	<sup>134</sup>
55	USA_TNO	SF	North America	35.97	-84.28	DBF	14.6	1497		1998-1999		clay	10.7	<sup>135</sup>
56	USA_TNP	SF	North America	35.96	-84.29	ENF	14.6	1489		1998-1999		clay	16.4	<sup>135</sup>
57	USA_WVF	SF	North America	39.06	-79.69	DBF	9.4	1408		1998-1999		loam	15.8	<sup>135,136</sup>





73 **Figure S10** – Fitted EF-SM relationship using a linear-plus-plateau model for the 43 Eddy-Covariance sites used in this  
 74 study. EF: evaporative fraction (-); SM: soil moisture (%).



75  
 76 **Figure S11** | Fitted Sapflux – soil moisture (swc\_shallow) linear-plateau relationship for an exemplary site containing 9  
 77 sapflux measurements (trees). Note that in Table S2 the site-specific median soil moisture threshold is reported (indicated by  
 78 the grey dot located at median  $\theta_{crit}$  and median sapflux density).

79

## 80 References

- 81 88. Beringer, J. *et al.* Special—Savanna Patterns of Energy and Carbon Integrated Across the  
 82 Landscape. *Bulletin of the American Meteorological Society* **92**, 1467–1485 (2011).
- 83 89. Cleverly, J. *et al.* Dynamics of component carbon fluxes in a semi-arid Acacia woodland, central  
 84 Australia. *Journal of Geophysical Research: Biogeosciences* **118**, 1168–1185 (2013).
- 85 90. Meyer, W. S., Kondrlovà, E. & Koerber, G. R. Evaporation of perennial semi-arid woodland in  
 86 southeastern Australia is adapted for irregular but common dry periods. *Hydrological Processes*  
 87 **29**, 3714–3726 (2015).

- 88 91. Hutley, L. B., Beringer, J., Isaac, P. R., Hacker, J. M. & Cernusak, L. A. A sub-continental scale living  
89 laboratory: Spatial patterns of savanna vegetation over a rainfall gradient in northern Australia.  
90 *Agricultural and Forest Meteorology* **151**, 1417–1428 (2011).
- 91 92. Cernusak, L. A., Hutley, L. B., Beringer, J., Holtum, J. A. M. & Turner, B. L. Photosynthetic  
92 physiology of eucalypts along a sub-continental rainfall gradient in northern Australia.  
93 *Agricultural and Forest Meteorology* **151**, 1462–1470 (2011).
- 94 93. Macfarlane, C., Prober, S. & Wiehl, G. FLUXNET2015 AU-GWW Great Western Woodlands,  
95 Western Australia, Australia, Dataset. *FLUXNET* <https://fluxnet.org//doi/FLUXNET2015/AU-GWW>  
96 (2013).
- 97 94. Beringer, J., Hutley, L. B., Tapper, N. J. & Cernusak, L. A. Savanna fires and their impact on net  
98 ecosystem productivity in North Australia. *Global Change Biology* **13**, 990–1004 (2007).
- 99 95. Beringer, J. *et al.* An introduction to the Australian and New Zealand flux tower network –  
100 OzFlux. *Biogeosciences* **13**, 5895–5916 (2016).
- 101 96. Beringer, J., Hutley, L. B., Hacker, J. M., Neininger, B. & Paw U, K. T. Patterns and processes of  
102 carbon, water and energy cycles across northern Australian landscapes: From point to region.  
103 *Agricultural and Forest Meteorology* **151**, 1409–1416 (2011).
- 104 97. Cleverly, J., Eamus, D. & Isaac, P. FLUXNET2015 AU-TTE Ti Tree East, Dataset. *FLUXNET*  
105 <https://fluxnet.org//doi/FLUXNET2015/AU-TTE> (2012).
- 106 98. Leuning, R., Cleugh, H. A., Zegelin, S. J. & Hughes, D. Carbon and water fluxes over a temperate  
107 Eucalyptus forest and a tropical wet/dry savanna in Australia: measurements and comparison  
108 with MODIS remote sensing estimates. *Agricultural and Forest Meteorology* **129**, 151–173  
109 (2005).
- 110 99. Arndt, S. K., Hinko-Najera, N., Griebel, A., Beringer, J. & Livesley, S. FLUXNET2015 AU-Wom  
111 Wombat, Dataset. *FLUXNET* <https://fluxnet.org//doi/FLUXNET2015/AU-Wom> (2010).
- 112 100. Yee, M. S. *et al.* A comparison of optical and microwave scintillometers with eddy covariance  
113 derived surface heat fluxes. *Agricultural and Forest Meteorology* **213**, 226–239 (2015).

- 114 101. Carrara, A., Janssens, I. A., Curiel Yuste, J. & Ceulemans, R. Seasonal changes in  
115 photosynthesis, respiration and NEE of a mixed temperate forest. *Agricultural and Forest*  
116 *Meteorology* **126**, 15–31 (2004).
- 117 102. Merbold, L. *et al.* Greenhouse gas budget (CO<sub>2</sub>, CH<sub>4</sub> and N<sub>2</sub>O) of intensively managed  
118 grassland following restoration. *Global Change Biology* **20**, 1913–1928 (2014).
- 119 103. Etzold, S. *et al.* The Carbon Balance of Two Contrasting Mountain Forest Ecosystems in  
120 Switzerland: Similar Annual Trends, but Seasonal Differences. *Ecosystems* **14**, 1289–1309 (2011).
- 121 104. Dietiker, D., Buchmann, N. & Eugster, W. Testing the ability of the DNDC model to predict  
122 CO<sub>2</sub> and water vapour fluxes of a Swiss cropland site. *Agriculture, Ecosystems & Environment*  
123 **139**, 396–401 (2010).
- 124 105. Shi, P. *et al.* Net ecosystem CO<sub>2</sub> exchange and controlling factors in a steppe—Kobresia  
125 meadow on the Tibetan Plateau. *SCI CHINA SER D* **49**, 207–218 (2006).
- 126 106. Changliang, S. FLUXNET2015 CN-Sw2 Siziwang Grazed (SZWG), Dataset. *FLUXNET*  
127 <https://fluxnet.org//doi/FLUXNET2015/CN-Sw2> (2010).
- 128 107. Gourlez de la Motte, L. *et al.* Non-stomatal processes reduce gross primary productivity in  
129 temperate forest ecosystems during severe edaphic drought. *Phil. Trans. R. Soc. B* **375**, 20190527  
130 (2020).
- 131 108. McGloin, R. *et al.* Energy balance closure at a variety of ecosystems in Central Europe with  
132 contrasting topographies. *Agricultural and Forest Meteorology* **248**, 418–431 (2018).
- 133 109. Prescher, A.-K., Grünwald, T. & Bernhofer, C. Land use regulates carbon budgets in eastern  
134 Germany: From NEE to NBP. *Agricultural and Forest Meteorology* **150**, 1016–1025 (2010).
- 135 110. Knohl, A., Ernst Detlef, S., Kolle, O. & Buchmann, N. Large Carbon Uptake by an Unmanaged  
136 250 year-old Deciduous Forest in Central Germany. *Agricultural and Forest Meteorology* **118**,  
137 151–167 (2003).
- 138 111. Drought 2018 Team & ICOS Ecosystem Thematic Centre. Drought-2018 ecosystem eddy  
139 covariance flux product in FLUXNET-Archive format - release 2019-1. (2019) doi:10.18160/PZDK-  
140 EF78.

- 141 112. Grünwald, T. & Bernhofer, C. A decade of carbon, water and energy flux measurements of an  
142 old spruce forest at the Anchor Station Tharandt. *Tellus B* **59**, 387–396 (2007).
- 143 113. Pilegaard, K., Ibrom, A., Courtney, M., Hummelshøj, P. & Jensen, N. O. Increasing net CO<sub>2</sub>  
144 uptake by a Danish beech forest during the period from 1996 to 2009. *Agricultural and Forest*  
145 *Meteorology* **151**, 934–946 (2011).
- 146 114. El-Madany, T. S. *et al.* Drought and heatwave impacts on semi-arid ecosystems' carbon fluxes  
147 along a precipitation gradient. *Philos Trans R Soc Lond B Biol Sci* **375**, 20190519 (2020).
- 148 115. Deirmendjian, L. *et al.* Hydro-ecological controls on dissolved carbon dynamics in  
149 groundwater and export to streams in a temperate pine forest. *Biogeosciences* **15**, 669–691  
150 (2018).
- 151 116. Granier, A. *et al.* The carbon balance of a young Beech forest. *Functional Ecology* **14**, 312–325  
152 (2000).
- 153 117. Bonal, D. *et al.* Impact of severe dry season on net ecosystem exchange in the Neotropical  
154 rainforest of French Guiana. *Global Change Biology* **14**, 1917–1933 (2008).
- 155 118. Gioli, B. *et al.* Comparison between tower and aircraft-based eddy covariance fluxes in five  
156 European regions. *Agricultural and Forest Meteorology* **127**, 1–16 (2004).
- 157 119. Wolf, S., Eugster, W., Potvin, C., Turner, B. & Buchmann, N. Carbon sequestration potential of  
158 tropical pasture compared with afforestation in Panama. *Global Change Biology* **17**, 2763–2780  
159 (2011).
- 160 120. Tagesson, T. *et al.* Ecosystem properties of semiarid savanna grassland in West Africa and its  
161 relationship with environmental variability. *Glob Chang Biol* **21**, 250–264 (2015).
- 162 121. Bagley, J. E. *et al.* The influence of land cover on surface energy partitioning and evaporative  
163 fraction regimes in the U.S. Southern Great Plains. *Journal of Geophysical Research: Atmospheres*  
164 **122**, 5793–5807 (2017).
- 165 122. Campbell, J. L., Sun, O. J. & Law, B. E. Disturbance and net ecosystem production across three  
166 climatically distinct forest landscapes. *Global Biogeochemical Cycles* **18**, (2004).



- 167 123. Baldocchi, D. D. *et al.* Predicting the onset of net carbon uptake by deciduous forests with  
168 soil temperature and climate data: a synthesis of FLUXNET data. *Int J Biometeorol* **49**, 377–387  
169 (2005).
- 170 124. Wang, Y. *et al.* Testing stomatal models at the stand level in deciduous angiosperm and  
171 evergreen gymnosperm forests using CliMA Land (v0.1). *Geoscientific Model Development* **14**,  
172 6741–6763 (2021).
- 173 125. Chu, H. *et al.* Representativeness of Eddy-Covariance flux footprints for areas surrounding  
174 AmeriFlux sites. *Agricultural and Forest Meteorology* **301–302**, 108350 (2021).
- 175 126. Merbold, L. *et al.* Precipitation as driver of carbon fluxes in 11 African ecosystems.  
176 *Biogeosciences* **6**, 1027–1041 (2009).
- 177 127. Peichl, M., Arain, M. A. & Brodeur, J. J. Age effects on carbon fluxes in temperate pine  
178 forests. *Agricultural and Forest Meteorology* **150**, 1090–1101 (2010).
- 179 128. King, G., Fonti, P., Nievergelt, D., Büntgen, U. & Frank, D. Climatic drivers of hourly to yearly  
180 tree radius variations along a 6 °C natural warming gradient. *Agricultural and Forest*  
181 *Meteorology* **168**, 36–46 (2013).
- 182 129. Vogel, T., Dohnal, M., Dusek, J., Votrubova, J. & Tesar, M. Macroscopic Modeling of Plant  
183 Water Uptake in a Forest Stand Involving Root-Mediated Soil Water Redistribution. *Vadose Zone*  
184 *Journal* **12**, vzt2012.0154 (2013).
- 185 130. Lüttschwager, D. & Remus, R. Radial distribution of sap flux density in trunks of a mature  
186 beech stand. *Ann. For. Sci.* **64**, 431–438 (2007).
- 187 131. Agudé, D., Poyatos, R., Rosas, T. & Martínez-Vilalta, J. Comparative Drought Responses of  
188 *Quercus ilex* L. and *Pinus sylvestris* L. in a Montane Forest Undergoing a Vegetation Shift. *Forests*  
189 **6**, 2505–2529 (2015).
- 190 132. Isarangkool Na Ayutthaya, S. *et al.* Water loss regulation in mature *Hevea brasiliensis*: effects  
191 of intermittent drought in the rainy season and hydraulic regulation. *Tree Physiology* **31**, 751–  
192 762 (2011).

- 193 133. Yi, K., Dragoni, D., Phillips, R. P., Roman, D. T. & Novick, K. A. Dynamics of stem water uptake  
194 among isohydric and anisohydric species experiencing a severe drought. *Tree Physiology* **37**,  
195 1379–1392 (2017).
- 196 134. Pangle, R. E. *et al.* Methodology and performance of a rainfall manipulation experiment in a  
197 piñon–juniper woodland. *Ecosphere* **3**, art28 (2012).
- 198 135. Wilson, K. B., Hanson, P. J., Mulholland, P. J., Baldocchi, D. D. & Wullschleger, S. D. A  
199 comparison of methods for determining forest evapotranspiration and its components: sap-flow,  
200 soil water budget, eddy covariance and catchment water balance. *Agricultural and Forest*  
201 *Meteorology* **106**, 153–168 (2001).
- 202 136. Tajchman, S. J., Fu, H. & Kochenderfer, J. N. Water and energy balance of a forested  
203 Appalachian watershed. *Agricultural and Forest Meteorology* **84**, 61–68 (1997).
- 204
- 205